IEEE Access
Multidisciplinary : Rapid Review : Open Access Journal

Received 2 April 2023, accepted 26 April 2023, date of publication 9 May 2023, date of current version 10 July 2023.

Digital Object Identifier 10.1109/ACCESS.2023.3274657

RESEARCH ARTICLE

Energy Demand Load Forecasting for Electric Vehicle Charging Stations Network Based on ConvLSTM and BiConvLSTM Architectures

FAISAL MOHAMMAD[1], DONG-KI KANG[1], MOHAMED A. AHMED[2], AND YOUNG-CHON KIM[1,3]

[1]Department of Computer Engineering, Jeonbuk National University, Jeonju 54896, Republic of Korea
[2]Department of Electronic Engineering, Universidad Técnica Federico Santa María, Valparaíso 2390123, Chile
[3]Smart Grid Research Center, Jeonbuk National University, Jeonju 561-756, South Korea

Corresponding author: Young-Chon Kim (yckim@jbnu.ac.kr)

This work was supported by the National Research Foundation of Korea (NSF) Grant through the Korean Government under Grant 2021R1I1A305872911.

ABSTRACT The electrification of transport has proved to be a breakthrough to uplift the sustainable and eco-friendly platform in the global sector in which electric vehicles (EVs) are considered indispensable. In particular, creating intelligent energy management in the power distribution system integrated with electric vehicle charging stations (EVCS) as a new entity is one of the most important challenging tasks. The implementation of the EVCS network infrastructure should facilitate the adoption of the spatiotemporal electricity demand for EVs. The intelligent decision for the transmission, distribution, energy allocation and charging station placement by the control center or central aggregator is only possible by correctly forecasting its usage, occupancy, and energy or charging demand. Techniques like data analytics have enabled to extract data from the EVCS on a daily basis to store and process all the recorded data. To overcome the above-mentioned challenges related to energy demand forecasting for EVCS network, this work proposes two encoder-decoder models based on convolutional long short-term memory networks (ConvLSTM) and bidirectional ConvLSTM (BiConvLSTM) in combination with the standard long short-term memory (LSTM) network. Data on energy demand from EVCS located in four different cities is used in the proposed models. All datasets are preprocessed to make them suitable for the multi-step time-series learning models in order to make the framework data-centric. The suggested architectures are built on the ConvLSTM and BiConvLSTM to extract the key features from the spatiotemporal data of the energy demand data of the EVCS distributed over the time and space. The predicted outcomes generated by the suggested strategy are compared with conventional deep learning models and traditional machine learning techniques.

INDEX TERMS Electric vehicle, electric vehicles charging station, energy demand forecasting, ConvLSTM, BiConvLSTM, EVCS dataset.

I. INTRODUCTION

Electric vehicles (EVs) have been considered as a promising candidate for reducing global CO_2 emissions and climate change. In this direction, electric power utilities have made EV charging programs as an integral part to aid with the regulation of CO_2 releases. EV charging takes place usually at home, workplace, or roadside public electric vehicle charging stations. Among the three categories, the publicly available charging station for EVs has reached 1.8 million in number across the world in 2021. Compared to other years, the growth of electric vehicle charging stations (EVCS) installations has been substantially slower during the pandemic created by COVID-19. The average yearly growth rate was nearly 60% between 2015 and 2020 in the case of China [1]. The modern power grid, interchangeably known as the smart grid,

The associate editor coordinating the review of this manuscript and approving it for publication was Junho Hong.

has become a collaborative platform of multiple technologies connected to a common network like renewable energy sources like wind turbines, photovoltaics, and EVs. It is the reinvention of how energy is generated, transmitted, and distributed, using multiple technologies to provide a reliable and cost-effective way. The smart grid has integrated many new actors, such as prosumers, consumers, and aggregators, each of them having an important role to play. This led to a transition from a rigid centralized system to a versatile decentralized system [2]. Further, the integration of EVs in the distribution network keeps on adding to the peak load consumption of the grid, if not checked on time can prove to be disastrous. In the survey Sun et al. [3] conducted with EV drivers, it was found that public charging stations were used by 80% of respondents the most of the time to recharge their vehicles. Most of the EVCS operate throughout the day to fulfill the battery of incoming EVs. The EVs need timely coordination with the electric vehicle supply equipment (EVSE), to regulate the charging process with ease and increase the EV owner's satisfaction. The increased density of the adoption of EVs in urban areas has made it challenging to minimize intermittency and instant energy consumption from the grid. Therefore, it has become crucial to estimate the energy consumption prior to building a new infrastructure for EVs. As the EV penetration rate increases, developing spatial-temporal EV charging-power demand models is needed. Predicting the demand ahead of time is important for the EVCS operator in order to regulate the supply-demand and manage the limited resources for charging. There is a very few ongoing research work that focuses on creating a framework to forecast the energy demand of the EVCS network.

In order to optimize the consumption from the power grid, the proper management of the demand supply in an efficient and secure manner is needed. In particular, forecasting the energy demand of the EVCS with the methods detailed in this work can offer highly valuable ways of decision-making for various stakeholders of the rising EV industry (e.g., EVCS operators, aggregators, and independent system operators). The independent system operators or the local aggregators have to schedule the production from the power grids in advance to avoid inflation in peak demand caused by the adoption of the EVs, which can lead to power outages [4].

Recent research works proved that high computing technologies with increased storage memory and processor speed have opened up many opportunities for artificial intelligence, big data, and the internet of things. Deep learning and machine learning have became the promising candidates for solving complicated problems in different domains, including healthcare, manufacturing, electricity, finance, security, transportation, education, social media, and many more. The development of the information and communication technology (ICT), along with the deep learning models and high-performance computing architectures has made it possible to collect, analyze, and preprocess the data from the smart grid to learn features from spatiotemporal data making a robust solution. One of the aforementioned applications is estimating power or energy usage, where deep learning architectures have produced cutting-edge work. Among the deep learning models encoder-decoder based architectures have been able to produce mindblowing results in case of machine translation, speech recognition, and time series application etc.,

This work aims to investigate the state-of-the-art and novel deep learning models based on encoder-decoder network architecture using convolutional long short-term memory networks (ConvLSTM) and bidirectional ConvLSTM (BiConvLSTM). The proposed encoder-decoder architectures consists ConvLSTM and BiConvLSTM based encoders in combination with LSTM based decoder to build the framework for EVCS energy demand forecasting. Four different open datasets have been used for training each model in order to achieve higher accuracy with good generalization and less error rate. These datasets cover all common formats of charging behaviour, usually in the public charging facilities. The porposed framework considers the fact that the EV users are mostly using the public fast charging facility in order to alleviate the longer charging durations. The main objectives of this work are as follows:

- Propose two different encoder-decoder model based on ConvLSTM structure namely ConvLSTM-BiLSTM and BiConvLSTM-LSTM. Standard ConvLSTM has the ability to capture the long and short-term memory of energy demand data sequences and comprises both temporal and spatial information. In case of BiConvLSTM structure that learns temporal properties in a cascaded and deeper way, i.e., the ConvLSTM units in the backward layer are built upon the forward layer, to exchange the information between units in both directions.
- In order to address the aforementioned difficulties, the proposed architectures are tested on four different EVCS datasets to achieve the generalization and scalability of the deep learning model.
- Validate the proposed models using a real dataset for low error rate and high accuracy compared to the conventional deep learning models.

II. RELATED WORK

A. EVCS COMMUNICATION INFRASTRUCTURE

Smart grids provide a well built infrastructure for the wired and wireless communications owing to the development of technologies and protocols like 5G, open charge point protocol (OCPP), etc. to support the EV mobility. Vehicle-to-everything (V2X) energy transfer takes place through the internet of electric vehicles (IoEV) platform. Charging start and end time varies according to EV user mobility statistics. IoEV will enable connectivity among EVCS. Figure 1 shows a schematic diagram for the IoEV which mainly consists of four layers for grid integration of EVs and EVCS. The vehicle layer comes first in which EVs are integerated with the EVCS at the time of parking in order to charge their batteries. In the

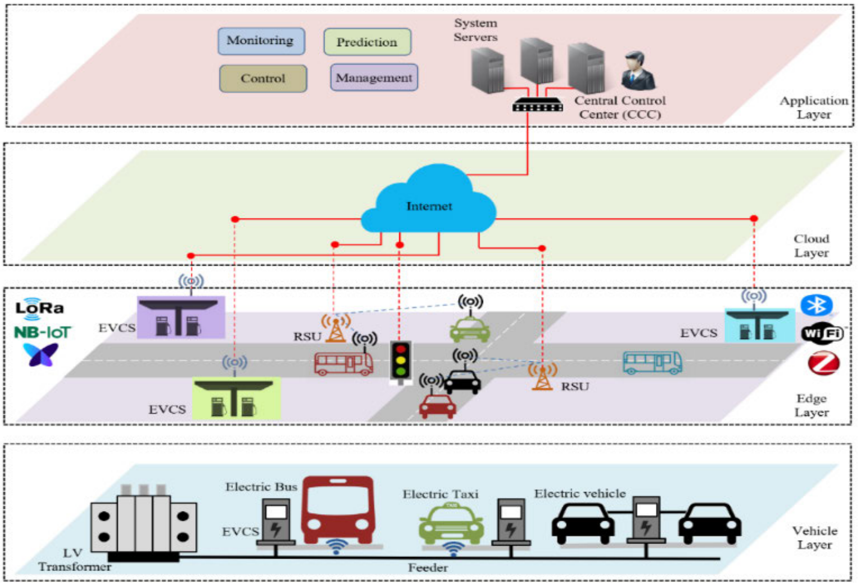

FIGURE 1. Schematic diagram for IoEV for grid integration of EVs and EVCS.

edge layer EVs communicate with road side units (RSUs) to wirelessly share their vehicle status information (VSI) whenever in need of charging. The central control center (CCC) collects, controls and manages the data received from the RSUs through the cloud layer. The CCC can be a utility company or load aggregator. During the EV charging session, the vehicle is connected to the charging station. Both vehicles and stations have to follow certain communication standards and protocols, established by the society of automotive engineers (SAE) [5].

The energy drained from the grid during the time between the start and finish of the charging session is the energy demand for an EV. The amount of load placed on the grid is determined by the EVCS charging mode, such as level 1 (slow charging) or level 2 (rapid charging), the charge duration, and the average parking duration, which varies widely across the EVCS network [6], [7].

B. ENERGY CONSUMPTION FORECASTING MODEL

A growing number of researchers are now interested in modeling EV charging using data-driven techniques. The summary of recent research on the energy demand forecasting for electric vehicle charging is shown in Table 1, which has been widely characterized based on modeling methodologies such as statistical, machine learning, deep learning, and reinforcement learning. In order to provide information and predictive analytics, the changing trends in EV customer's charging behavior has made an impact on the power generation and distribution [8]. Authors in [9] gave a comprehensive description of the methods that can be utilized to assess and forecast the charging behavior of EVs using supervised and unsupervised machine learning. Machine learning methods such as random forest algorithm proved to be the better prediction algorithm for charging station groups, which effectively tracks the estimated daily charging capacity of different charging stations based on the actual recorded data [10]. Lee et al. employed a bayesian inference learning to forecast the level of charge of the energy storage level of charge in hybrid electric vehicles [11].

For an accurate estimation of the energy consumption of electric vehicles, authors in [12] and [13] presented the use of machine learning techniques known as support vector machines. In order to anticipate the amount of energy used at the University of California's electric vehicle charging stations, Majidpour et al. [14] proposed time-weighted dot product (TWDP) dissimilarity measure to improve the accuracy and processing of the forecasting task. Forecasting the power consumption of the EV, [15], [16] came up with an emsemble technique. After surveying the traditional machine learning and statistical models, conventional approaches fail to offer forecasting models with a high predictive accuracy. As a result, deep learning techniques producing the state-of-the-art results in different domains including the time-series forecasting have been frequently applied to energy demand forecasting tasks [17], [18], [19], [20], [21].

In case of EVCS energy demand forecasting, the research is still in the progress to achieve the high accuracy. Long short-term memory, which is a recurrent neural network (RNN) based architecture, has been widely used to forecast the energy demand of the electric vehicle in the case of a single household or public charging station [22], [23], [24], [25]. In case of [26], the authors implemented empirical mode decomposition-arithmetic optimizer algorithm-deep long-short term memory on the EV charging dataset of Georgia Tech, Atlanta, USA. LSTM-based architectures have been often used to overcome the issue of vanishing and exploding

TABLE 1. Summary of the literature review regarding electric vehicle energy demand forecasting.

Reference	Year	Method	EVCS Dataset	Error Metric Used	Drawbacks	Advantages
[10]	2018	Random Forest (RF)	Shenzhen, China	Mean absolute percentage error (MAPE), Root mean square error (RMSE)	Data scarcity for the group of charging station, which lead to increase in the error as compared to the single charging station.	RF outperformed SVR and decision tree with lower error. Single station as well as group of stations were considered.
[11]	2019	Bayesian inference with Convolution	Household data	MAPE, RMSE	Single household dataset has been used with less number of features.	Flexible for variable trends against the linear regression model. Shorter forecasting horizon considered for 24 hours.
[12]	2014	Support Vector Regression (SVR)	Electric vehicle charging station in Shandong, China	MAPE	Selected features have to be known prior the start of the trip. Experiments have been conducted with a few vehicles over a long period of time.	The cloud-based approach using SVR-model used for the energy prediction got better accuracy and lower MAPE
. [14]	2015	Agent-based model using Clustering	Scottish and Southern Energy Power Distribution (SSEPD), UK	Relative Standard Deviation (RSD)	Limited dataset of only 19 EVs is considered.	The peak consumption for the clustered distributions against the random distributions are higher.
[15]	2022	NN-TWDP, MPSF, SVR, RF	UCLA campus, USA	Symmetric Mean Absolute Percentage Error (SMAPE)	EVCS records provide relatively slower prediction as compared to individual records concerning the customer privacy.	Predict the energy consumption in the next 24 hours of the EVCS at UCLA campus.
[16]	2019	Ensemble	Spanish Public Grid, Spain	Weighted Absolute Percentage Error (WAPE)	Ensemble outperformed the individual models like ARIMA and GARCH in the first hours with time it diminishes.	Model is robust and lower average error with seasons as the consumption trend changes.
[22]	2021	ARIMA, ANN, and LSTM	Korean Ministry of Environment, South Korea	MAPE	LSTM overall performed better but has the issue of overfitting and machine learning models attained less complexity but faced an issue of lower accuracy.	Three models were trained. results were presented in the geographical scales of a country, city, and single station using actual data.
[23]	2019	GRU	Shenzhen, China	Normalized RMSE and Normalized MAE	Single EVCS dataset for one year which is not enough to map the EV behaviour, thus can lead to model underfitting.	GRU worked well in case of hourly data of EVCS against its competitors DNN, LSTM, and RNN.
. [24]	2019	LSTM	Shenzhen, China	Mean absolute error (MAE), RMSE, and R^2	Single EVCS dataset for one year with only minute level forecasting.	LSTM model exhibits strongly competitive performance against its variants GRU and Bi-LSTM.
[25]	2021	LSTM	Jeju island, South Korea	RMSE, NRMSE, and NMAE	LSTM lacks the ability to map the distributed EVCS data over the entire to forecast.	LSTM model achieved good accuracy with RMSE of 61.63, NMAE of 5.15%, and NRMSE of 6.65% against Bi-LSTM, GRU, and RNN respectively.
. [26]	2022	LSTM	Georgia Tech, Atlanta, USA	MAE, RMSE, and MSE	Large number of deep layers were used which can increase time complexity of the model.	LSTM showed better results with the prediction accuracy of 97.14% with a very minimal MSE.
[27]	2022	LSTM with Bayesian Deep Learning	Caltech campus, California, USA	RMSE, MAE, Pinball, and Winkler	Employed to a single university campus EVCS network. Higher error value as compared to benchmark SVR.	LSTM-BDL outperformed other machine learning algorithms.
[29]	2020	Ensemble (ANN, RNN and LSTM)	Boulder, Colorado, USA	RMSE and MAE	Limited data is used and one-step ahead forecasting is considered.	Ensemble learning-based forecasting to reduce the error as compared to the baseline models.
[30]	2021	Ensemble (CNN and Queuing Model)	England, UK	RMSE, MAPE, and MSE	Focuses more on the traffic flow prediction and considers only fast charging station	Presented a traffic flow prediction model and introduced probabilistic model for EV charging load in CS using CNN and queuing ensemble model.
[32]	2021	Temporal Graph Convolution Network (T-GCN)	City of Palo Alto, USA	RMSE	Need to retrain the model for different horizons.	T-GCN model can capture the spatial and temporal correlations of the network of EVCS for multiple horizons.
[33]	2019	DNN with Federated Learning	EVCS data, Dundee city, UK	RMSE	Less focus has been made to decrease the forecast error.	Improved energy demand prediction accuracy and reduce the communication overhead in the EV network.
This work		ConvLSTM and BiConvLSTM	Palo Alto City and Boulder City (USA), Dundee City and Perth City (UK)	RMSE, MAPE, and MSE	Proposed model focused only in weekly forecast. Need to redefine the dataset for different horizons.	Outperformed other baseline models. The spatial and temporal correlations of the energy demand of EVCS network.

gradients of the standard RNN. Zhou et. al. proposed a methodological framework based on LSTM network combined with bayesian probability theory using EVCS data from the Caltech campus [27]. Similar approach has ben used in [28] on MID2008 survey open dataset for EV user mobility behaviors. In [29], charging data has been used for forecasting using ensemble LSTM with feed-forward neural network. Further, research has been done using the convolutional neural network in combination with queuing model to produce favourable results for EVCS demand forecasting [30]. In [31], the authors introduced a hierarchical probabilistic model based on Gradient boosted regression tree for electric vehicle load forecasting using the real data form Netherlands. Most of the above models are LSTM based which mostly deal with the temporal characteristics of the data but unable to tackle the issue of spatially distributed data. Hüttel et al. considered the both the spatio and temporal behavior of the EVCS data to increase the accuracy of the forecasting result which led them to propose the temporal graph convolutional networks [32]. To reduce the overhead of the communication in the EVCS network and timely update the forecasting model, the authors in [33] introduced the federated learning.

In case of spatio-temporal based models discussed use the EVCS data from a particular area which does not provide generalization capability. Similarly many other approaches were put to use for EV charging demand forecasting. Zhang et al. [36] introduced an extreme learning machine algorithm-based prediction-based optimal energy management of electric vehicles that also provided the driver torque demand forecast. Simultaneously, reinforcement learning is finding its way in demand forecasting, [37] provides a review of RL algorithms for EV charging management. While as [38] proposed Q-learning algorithm based approach to forecast the EVCS energy demand for multiple charging like uncoordinated, coordinated and smart.

Most of the forecasting models discussed in this section have the following shortcomings: First, the forecasting task circulates around the energy consumption of the individual EVs at residential places or a single EVCS, and few research works have focused on the city wide EVCS network energy demand consumption. Second, the traditional forecasting models lack the competency to deal with the spatiotemporal data of the energy demand of electric vehicle charging stations. The standard deep learning-based models, despite being good at handling temporal correlation, have too much redundancy for geographically dispersed data. When it comes to prediction, dealing with data simultaneously in both space and time coordinates is a challenging task. With the advancement in the LSTM based encoder-decoder architectures like ConvLSTM [39], [40], [41] and BiConvLSTM [42] proved to be the promising candidates for the forecasting tasks. The basic element of this architecture contains convolutional structures in both input-to-state and state-to-state transitions. This work uses the ConvLSTM-BiLSTM and BiConvLSTM-LSTM based encoder-decoder architectures to create better forecasting results than the standard models in order to address the issue of energy demand forecasting of EVCS network with the superior accuracy results.

C. DECISION VARIABLES FOR ELECTRIC VEHICLE CHARGING INFRASTRUCTURE

The penetration rate and grid integration of renewable energy sources (RES), including photovoltaic, energy storage systems (ESS), and EVs, continues to climb [43], [44]. With the changing trend of the energy management business model, an increasing number of energy consumers are making the shift to becoming energy prosumers. Energy prosumers have the option of using RES to generate some of the energy they require locally while distributing the excess to other consumers. Prosumer can support the electricity system at peak times when the grid energy cannot suffice the demand. By this way the participants can make the profit for themselves and avoid the power outages to a large extent. To make decisions more flexibly, a framework that can predict the future energy trend in the electric distribution system is required. Machine learning algorithms has paved a way to optimize the usage of the energy in a smart grid [44] with the help of forecasting.

1) ENERGY TRADING

The transactive energy market (TEM) is gaining greater attention as distributed energy resources (DER) deployments such as solar panels and battery energy storage systems and EV and EVCS integration on distribution networks increase. Authors in [46] determine TEM prices for energy trading amongst EVs at an EVCS housed inside office buildings with rooftop PVs using a dynamic pricing methodology. A management system for EV charging services in commercial buildings with on-site PV generating was presented in [47]. From the viewpoint of energy trading, EVs can exchange energy via vehicle-to-grid (V2G), grid-to-vehicle (G2V), vehicle-to-vehicle (V2V), and vehicle-to-home (V2H). In all the forms of charging, where energy traders can offer competitive prices to the EVs. Energy trading for EVs faces several difficulties, including those related to demand volatility, capacity and time volatility, customer satisfaction, fairness standards, privacy protection, battery, and energy consumption capacities, voltage and current instability caused by unexpected charging injection on the power system, pricing and frequency regulation issues, communication, and charging methods [48]. Therefore, forecasting the future demand of electric vehicles can lead to improved peer-to-peer energy trading.

2) CHARGING AND DISCHARGING SCHEDULING

For adequate and well-balanced energy consumption in charging stations with numerous entities, such as producers, consumers, and prosumers, an intelligent power management strategy must be put in place. The charging and discharge schedule of EVs is a crucial issue that needs to be addressed. It is fair for the EV or ESS to be charged during off-peak hours based on the hourly fluctuation of demand at the EVCS or smart home while considering the hours with low, average, and peak demand [49]. So, it makes sense that they charge when the total demand is low, depending on the need for electricity. Further, EV charging schedules need to be set according to the next day trip to avoid range anxiety [50]. On the other hand, the best times to discharge are during periods of high electrical demand. EVCS provides incentivization in charging/discharging costs in order to increase the advantages of EVCS for operators and EV owners by including customers in the efficient use of energy [51].

To tackle the uncertainty of geographically distributed temporal EVCS data, this paper proposes a spatio-temporal EV energy demand forecasting model for a public electric vehicle charging station network in a realistic traffic scenario. To the best of the authorsb knowledge, this article is the first attempt to investigate encoder-decoder architecture employing ConvLSTM and its variant BiConvLSTM techniques for predicting the energy demand of EVCS network. Four different electric vehicle charging station networks in four different cities are considered to analyze the performance, robustness, and generalization of the proposed EVCS demand forecasting model. In a single city, there are lot of EVCS which are geographically dispersed, this is due to the increasing penetration of the EV in that area (university campus, residential, market, etc), together with the timely use of the EVs throughout the day finally leads to the spatial distribution of energy demand data of the EVCS network. In order to incorporate spatial dependencies in addition to long-short term modeling, ConvLSTM replaces all of its linear operations with convolution layers. A ConvLSTM layer increases the spatial scale of the intermediate representations without affecting the global, long-term spatiotemporal properties of the data. This encoding happens throughout the LSTM's recurrent operation. The two properties are incorporated into a single ConvLSTM cell which gives it an upper hand over the other conventional deep learning models. While in case of BiConvLSTM the ConvLSTM units in the backward layer are built upon the forward layer. Thus, the forward ConvLSTM units share the sequential information with the backward layers. In proposed model, both ConvLSTM and BiConvLSTM has been cascaded with LSTM module to collect more spatial and temporal features, greatly enhancing the capacity of the ConvLSTM for temporal learning. In order to predict the EVCS future consumption the model should map the relationships between the input features and target with high precision. The more the predicted and actual energy demand values becomes closely correlate the good the proposed model is reliable and robust. The model algorithm is exclusively reliant on the data of the historical events, such as the arrival and departure of EVs, daily electricity consumption, etc.

III. ELECTRIC VEHICLE CHARGING STATION NETWORK DATASET

An intelligent communication system paves up new opportunities to develop and improve electric vehicles and mobility services, which makes mobility safer, more efficient, and more convenient. By seamlessly connecting users, electric vehicles, and services over the internet, drivers also get a fascinating experience leading to an increase in the smart data-driven technologies coming into existence, heightening the appeal of electromobility in general [52]. A high-quality dataset is essential for the development of strong artificial intelligence-based predictive models [53], [54], [55], [56]. As the EVCS datasets are usually time series dataset. Generally, time series dataset consists of multiple data points that are adjacent based on a specific time step. For the deep learning model training, four datasets are used. These datasets come from four different cities, namely Dundee and Perth in the United Kingdom (UK) and Boulder and Palo Alto in the

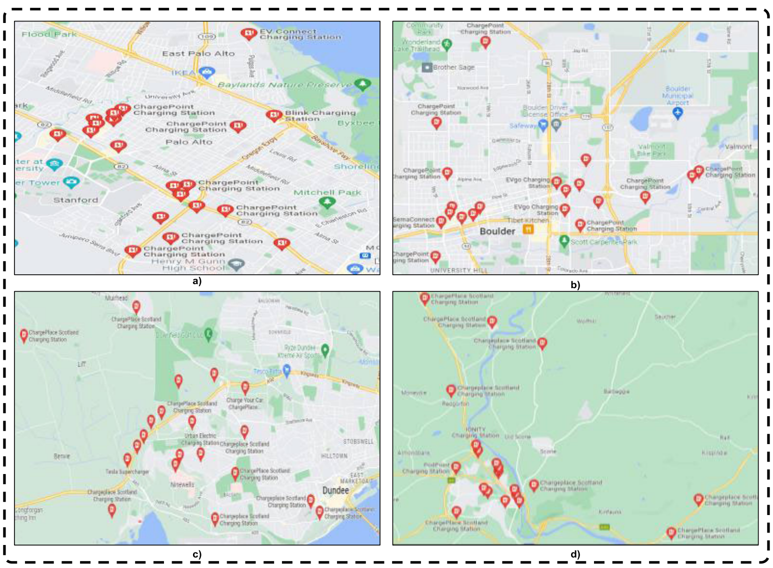

FIGURE 2. Electric vehicle charging station distribution in four different cities a) Palo Alto city b) Boulder city, c) Dundee city, and d) Perth city.

United States of America (USA). The fields shared across all these datasets are the session start and end times and the energy consumed in kilowatt hours. One more characteristic of these datasets is that they provide EVCS location, which can help in designing spatiotemporal models, as shown in Figure 2. All datasets used in this work have some specific attributes related to EVCS, EV, and charging event which are described below:

1. EVCS attributes: EVCS data includes an ID, name of the station, location address and area zip code. Further, it also has information like MAC address, latitude and longitude of the station, and each charging pile with the charging ports, either level 1, level 2, or DC fast charge.
2. EV attributes: EV share the information which containing a EV ID and registred zip code (which is usually the zip code of the driver's residence).
3. Charging event data: includes the start date and time of the charging event, end date and time of the charging event, charging duration, average stay duration, initial state of charge (SOC), final SOC, transferred energy, Greenhouse Gas (GHG) saving, and information on how was the charging event ended (e.g., terminated by customer or server).

A. PALO ALTO DATASET

The Palo Alto dataset contains various metadata on the charging transaction given in Appendix. Figure 2a shows the distribution of the EV charging stations over the Palo Alto using the Google maps based on the address, longitude, and latitude fields of the dataset [57]. It also consists of EV charging transactions at those locations. The dataset spans from 2011 to 2013, having 10000 transactions with 28 fields. The energy demand (kWh) for a charging event is minute based, which is the target to predict. The energy demand is aggregated into a daily energy demand for each of the stations in Palo Alto.

B. BOULDER DATASET

The City of Boulder dataset has 48 public EVCS located at city facilities, the recreation centers and downtown parking garages [58]. Appendix, Table 3 provides the description of the dataset consisting of 12 fields with total of 36,326 charging transactions. Figure 2b depicts the distribution of EV charging stations locations in the City of Boulder. The dataset ranges from January 2018 to November 2021. EV charging stations are distributed over the City of Boulder using the address field of the dataset by employing Google Maps.

C. DUNDEE DATASET

A modern and effective EV fleet will be deployed around the city as part of a smart city project led by Dundee City Council [59]. Through close collaboration with the Scottish Electric Vehicle Association (EVAS) and its members, Dundee has already made its public charging stations available. The real data obtained from 58 electric vehicle charging stations situated in Dundee city, Scotland, during 2017 and 2018. The actual data collected from these stations between those years was accurate. In particular, the

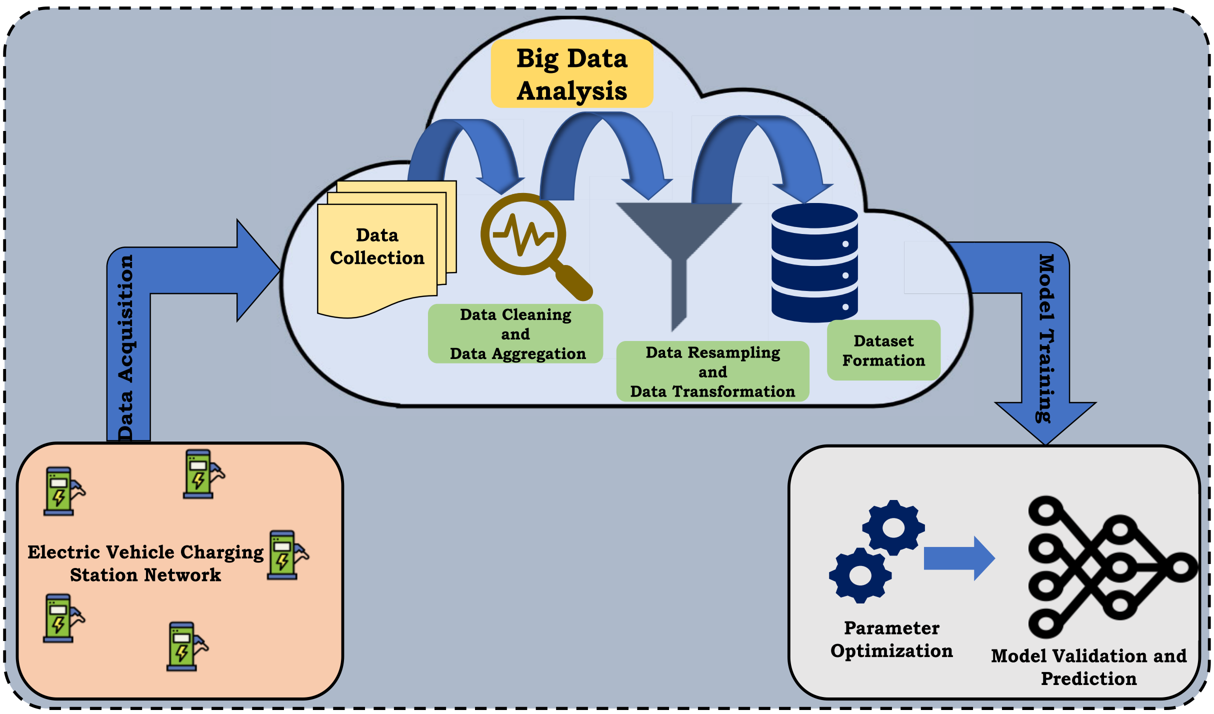

FIGURE 3. Proposed framework of the EVCS charging demand forecasting system.

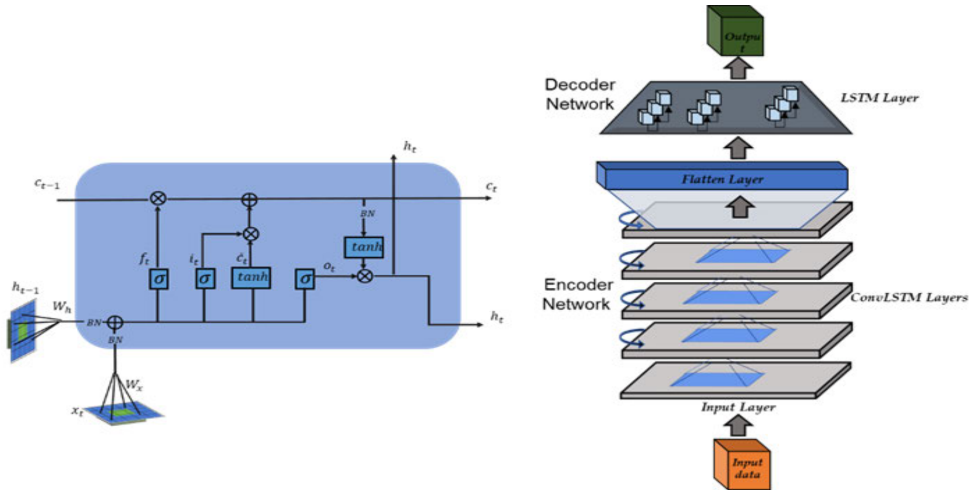

FIGURE 4. Architecture of the ConvLSTM cell and ConvLSTM layers stacked in an encoder network stacked in an encoder network.

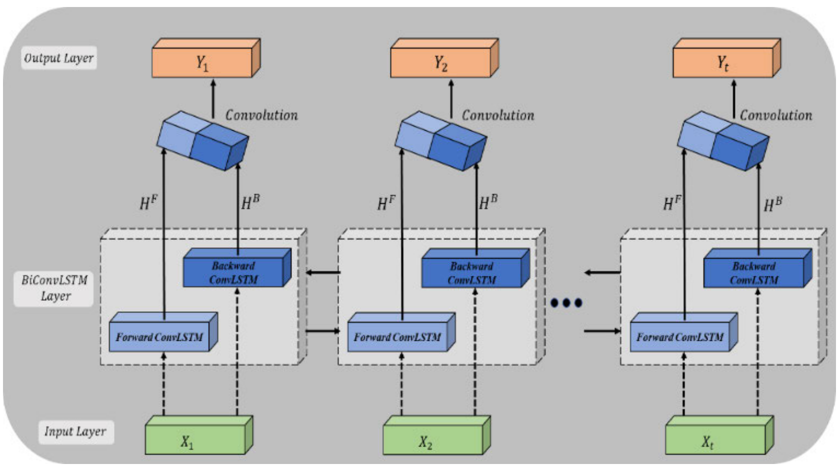

FIGURE 5. Overview of the BiConvLSTM Cell.

dataset has 52,475 transactions. Table 3 in Appendix shows the detailed description of the dataset which includes identification number, transaction ID for each EVCS, EV charging date, EV charging time, and consumed energy (kWh). Figure 2c shows the distribution of the EV charging stations over the City of Dundee based on the address field of the dataset.

D. PERTH DATASET

EVCS located around the Perth city as shown in figure 2d, which are under the ChargePlace Scotland scheme. The Perth dataset includes anonymous data from each individual charging session. It consists of three years data ranging from January 2016 to December 2019. Each row has 10 fields with a total charging session of 66,665. It has 41 electric car charging points at the Broxden Park and Ride including rapid chargers as well as fast chargers. Charge Place Scotland will soon offer differential tariffs which will attract the EV customers to take advantage of cheaper off-peak energy usage and also allow more targeted overstay fees that would allow users to charge their EV during the night without amounting penalty fees [60]. Description is given in Table 3 Appendix.

IV. PROPOSED FRAMEWORK

The future smart power grid needs to understand the flexibility potential of assets like EVs and other intermittent resources in order to coordinate the operation between the producers, consumers, and prosumers. This section proposes an ideal forecasting model to address the aforementioned issue and enhance the forecasting accuracy. In order to construct a forecasting model, many elements must be addressed, such as the quantity of data, the input covariates and output target variable, the choice of algorithm, etc. The publicly accessible datasets that give information on EV charging sessions. The task of load forecasting is made simpler by the big number and the well-engineered data [61].

In this work, an energy demand forecasting framework is proposed to build an efficient energy management system for electric vehicles in order to create optimal schedule charging transactions considering the constraints of the power grid. Figure 3 illustrates the framework of the proposed EVCS energy demand forecasting model. The framework consists of the following modules:

i. EVCS infrastructure
ii. Energy demand forecasting model for EVCS network
iii. Middleware layer: EVCS Big Data Analysis
iv. Application layer: Model Training and Prediction

A. ELECTRIC VEHICLE CHARGING STATION NETWORK INFRASTRUCTURE

In recent years, it has become more crucial to take into account intelligent charging algorithms and various uses of EV batteries for auxiliary service offering. In order to collect the data from a smart EVCS network and since EVs are a variable resource, having a reliable and adequate charging infrastructure is crucial. The highest amount of energy delivered per public EVCS with a specific power capacity is described by usage. Thingvad [62] provides a useful summary of the energy and charging infrastructure required. Similarly, in [63], the authors provided an overview explaining the EVCS infrastructure, EV mobility, and charging behaviour. The availability of public charging infrastructure benefits intercity travel, emergency fast charging, and EV owners who cannot set up charging stations at home. Additionally, public charging stations can assist EV users in overcoming range anxiety when traveling long distances. Further, the developments in information technology and communication data generation, data processing, and control are transforming the transportation sector from model-driven systems into data-driven intelligent transportation systems (ITS). The data-driven model provides a hands-on solution using artificial intelligence.

B. ENERGY FORECASTING MODEL FOR EVCS NETWORK

Machine learning and its derivative deep learning are currently contending with one another to improve accuracy and decrease error rates for tasks involving classification or regression. Given the high degree of uncertainty and dynamic nature of the data on EV power usage, forecasting tasks must effectively address these fundamental problems. Inaccurate input-to-target mapping results from uncertainty, particularly for statistical or linear models. Due to the non-linear nature of the energy data, deep learning models offer a strong architecture to deal with this randomness. Encoder-Decoder based deep learning model proved to be one the promising architecture to be used in time-series forecasting. In this paper, two state-of-the-art encoder-decoder architectures are employed. The spatiotemporal encoding is done using two different encoders based on standard ConvLSTM and its variant BiConvLSTM. The decoder part consists of standard LSTM architecture. The architectures for both encoders and decoders are described below.

1) SPATIOTEMPORAL ENCODER ARCHITECTURE

2) CONVOLUTIONAL LONG SHORT-TERM MEMORY

A ConvLSTM layer learns spatiotemporal dependency in the time-series energy consumption dataset. The encoder network consisting of ConvLSTM is used to fully analyze spatiotemporal correlation information by utilizing the convolution and recurrence operations as compared to simple LSTM. The ConvLSTM layer can regain the lost spatial information along with the temporal representations during the training. Convolution and recurrence operations are used for both input-to-input and state-to-state transitions making the final state have a large receptive field. Figure 4 shows the internal cell structure of the ConvLSTM, and the placement of ConvLSTM layers in the encoder-decoder architecture, which receives the input data through the input layer and forwards it to the encoding layers which is then transferred to the decoding layer via flattening layer to produce the forecasting results. The ConvLSTM model was first introduced to study precipitation nowcasting [39].

ConvLSTM consists of an input gate i_t, an output gate o_t, a forget gate f_t, and a memory cell C_t. These gates act as controlling pathways to access, update, and clear memory cell. Equation (1)-(6) defines the operations in the ConvLSTM network:

$$i_t = \sigma(W_{xi} * X_t + W_{hi} * H_{t-1} + W_{ci} \circ C_{t-1} + b_i) \quad (1)$$
$$f_t = \sigma(W_{xf} * X_t + W_{hf} * H_{t-1} + W_{cf} \circ C_{t-1} + b_f) \quad (2)$$
$$\tilde{C}_t = tanh(W_{xc} * X_t + W_{hc} * H_{t-1} + b_c) \quad (3)$$
$$C_t = f_t \circ C_{t-1} + i_t \circ tanh(W_{xc} * X_t + W_{hc} * H_{t-1} + b_c) \quad (4)$$
$$o_t = \sigma(W_{xo} * X_t + W_{ho} * H_{t-1} + W_{co} \circ C_t + b_o) \quad (5)$$
$$H_t = o_t \circ tanh(C_t) \quad (6)$$

where X_t denotes the input of the current cell, C_{t-1} and H_{t-1} are state and output of the last cell, respectively. '$*$' denotes the convolution operation and '$\circ$' denotes the Hadamard product. $W_\bullet$, $W_\bullet$, $W_\bullet$ denotes the 2-D convolution filters with a $k * k$ kernel size. The definitions of, b_i, b_f, and b_o are similar to that of simple LSTM architecture, however, the data dimensions and processing methods are different. When the training of ConvLSTM begins as the input arrives, the new data will be accumulated to the memory cell C_t if the input gate i_t is activated. Similarly, the past cell status C_{t-1} could be forgotten if the forget gate f_t is switched on. Whether the latest memory cell's value C_t will be transmitted to the final state H_t is further controlled by the output gate o_t. ConvLSTM can extract a more useful feature representation than CNN due to this unique structure. Additionally, in comparison to LSTM, the three gate mechanism implementations use 3D tensors to expand from one-dimensional to multi-dimensional convolution operation.

3) BIDIRECTIONAL CONVOLUTIONAL LONG SHORT-TERM MEMORY

The word bidirectional depicts the two directions, forward direction and backward direction. The BiConvLSTM used in this work is the enhancement to the standard ConvLSTM. In [40], the work provides a detailed description of the BiConvLSTM architecture and its application for object detection in video frames. The concept is similar to that of bidirectional LSTM in which the input flows in the both directions and has the potential of utilizing information from both sides. In case of BiConvLSTM the ConvLSTM units in the backward layer are built upon the forward layer to capture the temporal characteristics in both directions as shown in Figure 5. This cascaded layer architecture makes it possible for the forward ConvLSTM units to exchange their sequential knowledge with the backward layers. BiConvLSTM architecture is expressed in the following equations:

$$i_t^B = \sigma(W_i^{H^F} * H_t^F + W_i^{H^B} * H_{t+1}^B + b_i) \quad (7)$$

$$f_t^B = \sigma(W_f^{H^F} * H_t^F + W_f^{H^B} * H_{t+1}^B + b_f) \quad (8)$$

$$o_t^B = \sigma(W_o^{H^F} * H_t^F + W_o^{H^b} * H_{t+1}^b + b_o) \quad (9)$$

$$C_t^B = f_t^B \circ C_{t+1}^B + i_t^B \circ \tilde{C}_t \quad (10)$$

$$\tilde{C}_t = tanh(W_c^{H^F} * H_t^F + W_C^{H^B} * H_{t+1}^B + b_C) \quad (11)$$

$$H_t^B = o_t^B \circ tanh(C_t^B) \quad (12)$$

The final output considering bidirectional spatiotemporal information is given by Equation as follows:

$$Y_t = tanh(W_y^{H^F} * H_t^F + W_y^{H^B} * H_{t-1}^B) \quad (13)$$

where $\boldsymbol{H^F}$ and $\boldsymbol{H^B}$indicates the hidden states from forward and backward ConvLSTM units, and $\boldsymbol{Y_t}$ indicates the final output considering bidirectional spatiotemporal information. The ConvLSTM units in the forward layer receive spatial feature maps $\{\boldsymbol{X_t}\}_{t=1}^{\boldsymbol{T}}$ from T frames as inputs, and output forward sequential feature maps $\{\boldsymbol{H_t^F}\}_{t=1}^{\boldsymbol{T}}$ according to Eq. 1-6. The deeper layer is constituted of the backward units that receive the output features from the forward layer $\{\boldsymbol{H_t}\}_{t=1}^{\boldsymbol{T}}$ as inputs. Then the forward features $\{\boldsymbol{H_t^F}\}_{t=1}^{\boldsymbol{T}}$ and the backward features $\{\boldsymbol{H_t^B}\}_{t=1}^{\boldsymbol{T}}$ are combined for final outputs: $\{\boldsymbol{Y_t}\}_{t=1}^{\boldsymbol{T}}$ using Eq. 11. In this way, information is encouraged to flow between the forward and backward ConvLSTM units, and deeper spatiotemporal features can be extracted by the backward units.

In a standard ConvLSTM, the dependencies of the forward direction are processed. However, all the information in a sequence should be fully considered, therefore, it might be effective to consider backward dependencies. It has been proved that analyzing both forward and backward temporal perspectives enhanced the predictive performance.

4) TEMPORAL DECODER ARCHITECTURES

a: LSTM

The LSTMs are specifically designed RNN based architecture to support sequences of input data and has solved the problem of vanishing or exploding gradients of the conventional RNN. Modeling long-range relationships successfully involve learning the intricate dynamics of the temporal ordering of sequential input using an internal memory. Figure 6 representes the unrolled structure of the standard LSTM cell. The LSTM can be configured into an encoder-decoder architecture, enabling the model to be applied to both variable length input sequences and the generation of variable length output sequences over a temporal range. Contribution of LSTM is recurrent connections, memory cell C_t, and the self parameterized and controlling gates, which essentially control the flow of the state information. LSTM as a temporal decoder takes the input from the encoder as time series data. In encoder part, the entire input sequence, the hidden state or output of encoder model represents an internal learned representation as a fixed-length vector. This vector is then provided as an input to the LSTM decoder model that interprets it as the output sequence. LSTM decoder network finally outputs a 3D vector with the same input sequence of dimensions as [*samples, timesteps, features*].

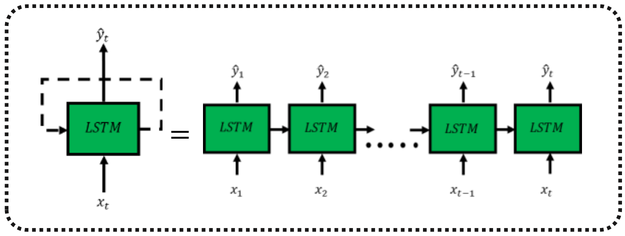

FIGURE 6. Standard LSTM cell unrolled.

b: BIDIRECTIONAL LSTM

One of the variants of the conventional LSTM is bidirectional long Short-Term Memory (BiLSTM), one of the recurrent neural networks, which can process both past and future information, whereas traditional LSTMs can only do with one-way transmission of information. The working principle of BiLSTM is that the same output connects two LSTM networks with opposite timings. Figure 7 shows the BiLSTM architecture's unrolled structure. The forward LSTM can receive the input sequence's past data information, while the reverse LSTM can obtain the input sequence's future data information. Each level of the bidirectional LSTM network gives the forward and backward layer output to the activation layer, a neural network, and the output of this activation layer is taken into consideration. This output also includes information about or a relationship between past and future datapoints. The hidden state $\boldsymbol{H_t}$ of BiLSTM at time t includes two sets forward $\boldsymbol{H_t^F}$ and backward $\boldsymbol{H_t^B}$. The BiLSTM is mathematically expressed as follows:

$$H_t^F = LSTM(H_{t-1}, X_t, C_{t-1}) \quad (14)$$

$$H_t^B = LSTM(H_{t+1}, X_t, C_{t+1}) \quad (15)$$

$$H_t = [H_t^F, H_t^B] \quad (16)$$

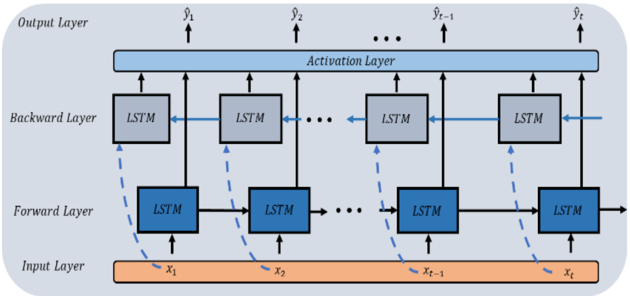

FIGURE 7. An overview of bidirectional LSTM.

C. PROPOSED DEEP LEARNING ARCHITECTURE

Although fully connected standard LSTM can single handedly deal with the temporal characteristics of the timeseries data but is unable to read the spatial attributes. To address this issue, two encoder-decoder based architectures are proposed which can efficiently deal with the spatiotemporal correlation of the timeseries data [64].

1) ConvLSTM AND BiLSTM BASED ENERGY DEMAND FORECASTING MODEL

ConvLSTM is an improvement over traditional LSTM that uses convolutional structures to read the spatiotemporal nature of input-to-state and state-to-state transitions. Two networks, an encoding network and a forecasting or decoding network, have been built to solve the spatiotemporal sequence forecasting problem as shown in Figure 8. The initial states and cell outputs of the forecasting network are copied from the last state of the encoding network using the flatten layer and repeat vector layer. The enhanced design of ConvLSTM is that the gates, cell state, hidden state, and inputs $X_1, X_2, \ldots, X_t$ are changed to 3D tensors with the last two dimensions as spatial. The encoder network determines the future state of a 3D cell using the inputs and the past state information of its neighbouring cells by virtue of the convolution operator.

In this architecture, the encoder module is made up of ConvLSTM layer to gain consistency in knowledge about the spatial behaviour of the data, while as the decoder module consists of bidirectional LSTM. The feature maps produced by the ConvLSTM are forwarded to the flatten layer to reorder them from the spatial dimensions to one dimensional array that can then be used as input to the decoding process. This 1D array is reproduced into a 2D array by passing via the repeat vector layer. For each time step in the output sequence, the internal representation of the input sequence is iterated over many times. The LSTM decoder will be shown this series of vectors.

The input layer takes the data, which is then transferred to the ConvLSTM layer. After the data preprocessing step, the timeseries EVCS network data is fully polished as the input data to train the model. The ConvLSTM encoder input layer receives the input data in the shape of a tuple $[n, t, r, c, ch]$ where

- n samples
- t timesteps
- r number of rows
- c number of columns
- ch channels.

The input matrix is one-dimensional sequence of total power consumption, which can be interpreted as one row with 7 or 14 columns, depending on what amount of datapoints are taken as input to make the forecast. Each timestep of data is defined as an image of dimension $r*c$. In the encoder part, there is one ConvLSTM layer which is equipped with 1×3 kernels having a total number of kernels or filters of 64 and the activation function is set as rectified linear unit (*ReLU*).

The encoder block can have one or more ConvLSTM layers stacked depending upon the model selection, therefore, in the later section, we have provided an intensive ablation study for choosing the number of layers and other hyperparameters. To connect the encoder and decoder blocks, there are flatten layer and repeat vector. The *RepeatVector* layer regenerates the input to produce the output with the dimensions of [*1, 7, 1*] which is passed to decoder part. The deoder has three BiLSTM layers and each BiLSTM layer consists of 200 units of neurons with *ReLU* activation function. Further, in the decoder part $L2$ regularization is employed which is also known as kernel-regularizer, to improve the accuracy of the model. After that, an fully connected layer is placed to interpret each time step in the output sequence prior to the final output layer, which could be just a single step. There should be seven sequential values for a week prediction. It means that each time step provided by the decoder will be processed using the same fully connected layer and output layer. In order to achieve this, the interpretation layer and output layer must be wrapped in a time-distributed, fully connected wrapper that enables the wrapped layers to be used for each time step from the decoder.

2) BiConvLSTM AND LSTM BASED ENEGY DEMAND FORECASTING MODEL

The BiConvLSTM and LSTM is an encoder-decoder architecture consisting of single BiConvLSTM in the encoding layer and two stacked LSTM layers in the decoding module as shown in Figure 9. Optimal number of layers and number of neurons in each layer has been verified by doing multiple experiments. This enhancement of the ConvLSTM is done to verify the applicability of the BiConvLSTM in the case of energy demand forecasting. BiConvLSTM can be considered as of the forward and backward standard ConvLSTM. Therefore, it has two sets of training parameters for backward state and forward state respectively. The equations in the section C, II ellaborates the structure and the flow of the information in the BiConvLSTM cell.

D. MODEL TRAINING AND PREDICTION

In this work, our focus is to provide a weekly forecast, therefore, the forecasting horizon will be the daily aggregate energy consumption of EVCS network in a particular

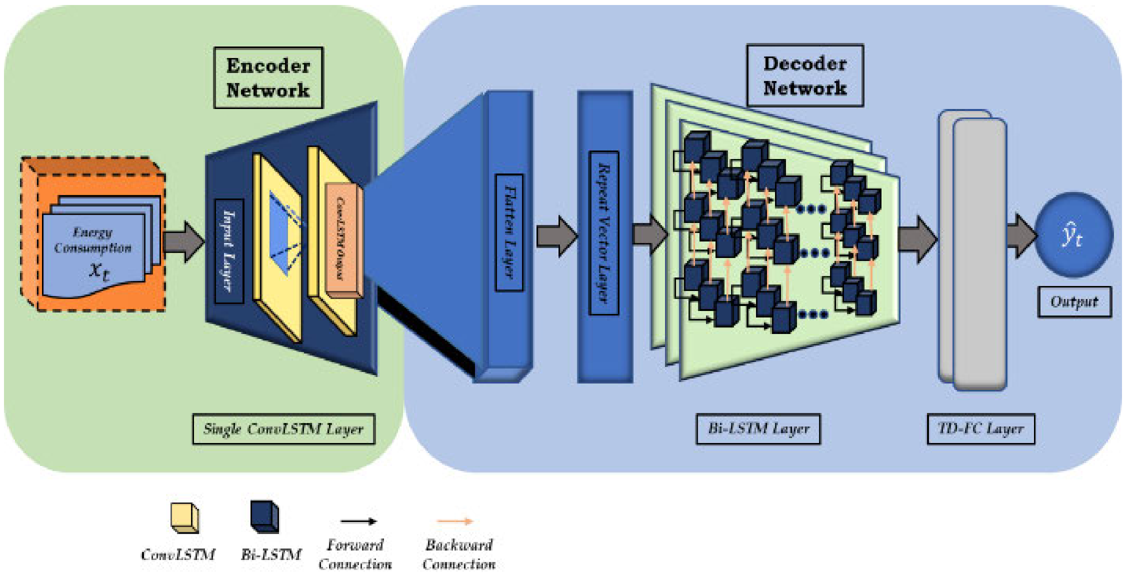

FIGURE 8. ConvLSTM and BiLSTM based encoder-decoder architecture for EVCS energy demand forecasting.

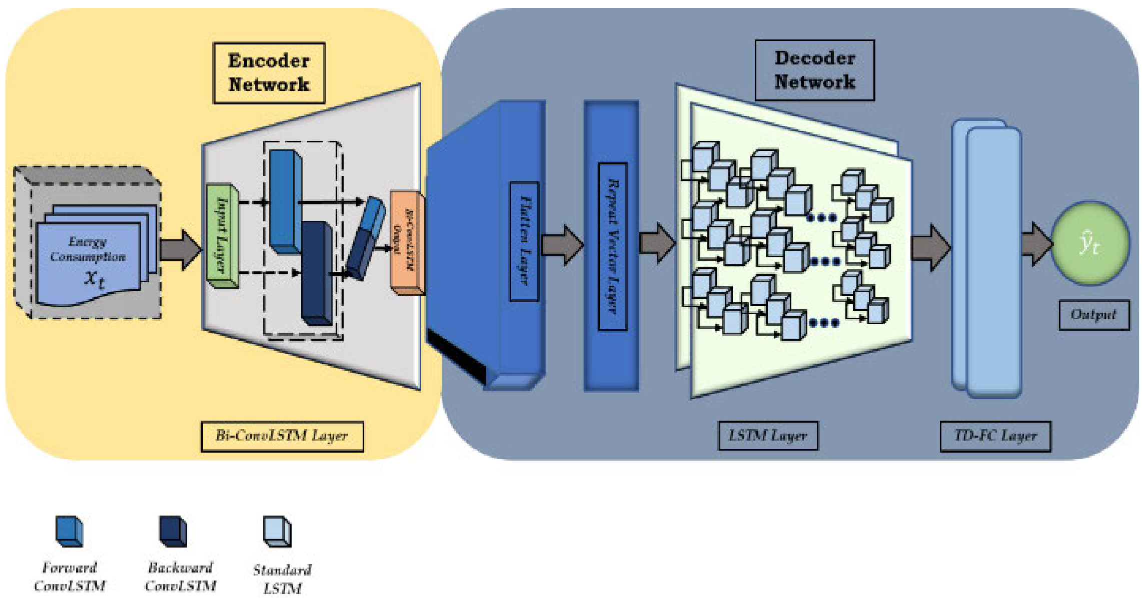

FIGURE 9. BiConvLSTM and LSTM based encoder-decoder architecture for EVCS energy demand forecasting.

area. The data should be separated into normal weeks, each of which starts on sunday and ends on saturday. This is a practical and realistic technique to apply the model's selected framework, allowing for the prediction of the coming week's power consumption. It is useful during modeling, as models may be used to forecast a certain day of the week or the entire series. Working backwards from the training dataset, the split method is used to divide the data into standard weeks. We must manually choose a dataset length that can be a multiple of seven in order to divide the entire number of datapoints into standard weeks if the datapoints are not automatically separated into weeks. Restructuring of the final dataset into train and test data is done using the split function, which takes start and end index of the train and test sets. The most effective deep learning architecture for the EVCS energy demand forecasting task is determined by the selection of neural network hyperparameters, including the batch size of the training set, number of hidden layers, activation function in the hidden layers, dropout, optimization algorithm, number of training epochs, etc.

In the case of *ConvLSTM* + *BiLSTM* based architecture, the encoder network has multiple ConvLSTM layers stacked over one another. Similarly, in the decoder network side, multiple BiLSTM layers are put to play. We choose a single ConvLSTM layer in the encoder network and three cascaded BiLSTM layers in the decoder network, which outperforms other competing model architectures for energy demand forecasting task. In the encoder network, the ConvLSTM operates over the data by considering it as an image and convolves over it spatiotemporally, and the final output in the form of feature map is then passed to a flatten layer. The flatten layer outputs 1D vector of length 1536 which is passed as input to *RepeatVector* layer which produce the output of matrix 7 $\times$ 1536. The output is now an input to the decoder network which consists of BiLSTM layers. The BiLSTM layer performs operations over the input following the equation in section II. The output of the decoder layer is fed to the first $TimeDistributed - FullyConnected$ layer having 100 hidden neurons and then to the second TD-FC layer having one neuron to produce the prediction result of the energy demand of a single day which is aggregated with other consecutive six outputs to give the final forecasting result of the whole week.

In the case of $BiConvLSTM - LSTM$ architecture, we choose single BiConvLSTM in encoder network and two layers LSTM in the decoder network as model architecture for the energy demand forecasting task. During the training process, we simultaneously employed multiple architectures to validate the performance in terms of error rate by using loss function called MSE. The BiConvLSTM does the same work but in the both directions because it comprises of ConvLSTM block with two sets of the hidden state H_t^F, H_t^B and cell state C_t^F, C_t^B. The (H_t^F, C_t^F) is for the forward pass and (H_t^B, C_t^B) is for the backward pass. The model can make predictions using the fit model. There is not any fixed way to select the optimal number of layers in both encoder and decoder, we just use random way by comparing the error using the loss function called mean square error (MSE). Section V provides the ablation study and list the performance when different variants of this model are employed. In decoder network, multiple LSTM layers are stacked and each LSTM layer has the activation function ReLU. We use the walk forward validation method to validate the model, which is similar to the k-fold cross validation [65]. In order to prevent the model from becoming overfit, this approach forecasts at each time step using a sliding window methodology. In order to accelerate training, we used two alternative regularization techniques. The first is dropout, which leaves 50% of the hidden neurons untrained in order to simplify the model. L2 regularization, commonly known as Ridge Regression, comes in second. L2 regularization is set at 0.001 by default. The model is trained for 100 epochs with different batch sizes of 32, 64, 128, and 256 using the Adam optimizer. Finally, after continuous experimentation, the batch size of 64 has been selected as it provides the better results in terms of loss function and time complexity. Variable batch size affects the training time of the deep learning model, smaller batch takes a long time to train, while as larger batch size takes less time.

To evaluate the performance of a specific model, we calculate the average loss value of that model.

V. PERFORMANCE EVALUATION

A. PERFORMANCE METRICS

1) MEAN SQUARE ERROR

The mean absolute error calculates the mean of the absolute differences between the predicted energy demand $\hat{y}(i)$ and the actual energy demand $y(i)$ over the whole dataset of N samples. The MSE actually measures the average of the squares of the error. It strictly gives a positive value that decreases as it tends to approach zero.

$$MSE = \frac{1}{N} \sum\nolimits_{i=1}^{N} \left[y(i) - \hat{y}(i)\right]^2 \tag{17}$$

2) MEAN AVERAGE PERCENTAGE ERROR

Mean average percentage error is a measure of the prediction accuracy of a forecasting method in the statistical analysis of the dataset. It is the most commonly used error metric to measure the performance of the model. Since it depicts the value in percentage, which makes it always positive, it usually expresses the accuracy as a ratio defined by the formula:

$$MAPE = \frac{100}{N} \sum\nolimits_{i=1}^{N} \left|y(i) - \hat{y}(i)/y(i)\right| \tag{18}$$

In the above equations $y(i)$ is the actual or real value, $\hat{y}(i)$ is the predicted value, and N is the total number of samples.

3) ROOT MEAN SQUARE ERROR

The root mean square error is also sometimes called root mean square deviation (RMSD). It represents the square root of the differences between predicted energy values $\hat{y}(i)$ and actual energy values $y(i)$ or is the square root of the average of squared errors over the whole dataset of N samples. The RMSE is a single indicator of predictive power that combines the sizes of predictions errors for numerous data points. RMSE is a metric for accuracy that may be used to evaluate forecasting mistakes across many models for a given dataset.

$$RMSE = \sqrt{\frac{1}{N} \sum\nolimits_{i=1}^{N} \left[y(i) - \hat{y}(i)\right]^2} \tag{19}$$

B. EVCS BIG DATA ANALYSIS

Like drivers of conventional cars known as internal combustion engine vehicle (ICEV), all EV drivers have comparable driving habits. Transiting from an ICEV to an EV shouldn't significantly alter regular travel patterns. Daily trip from home to work or to shopping centers remains same. Electric vehicle charging stations network in each city considered in this work follows similar trend in case of energy consumption. The dataset from the city of Palo Alto, which spans a period of six years, is followed by those from Perth, which spans four years, Boulder, which spans just over two years, and Dundee, which spans two years. The data analysis is processed using the following steps:

TABLE 2. Average results forecasting performance of proposed models versus other state-of-art models in terms of RMSE, MAPE, and MSE.

Dataset	Metric	LSTM	CNN	CNN + LSTM	LSTM + LSTM	BiLSTM + BiLSTM	*proposed model I*	*proposed model II*
Palo Alto	RMSE	0.927	0.931	1.085	1.157	0.889	**0.71**	0.73
	MAPE	282.03	215.44	235.6	251.3	198.63	**183.16**	245.81
	MSE	1	0.89	1	0.93	0.99	0.878	**0.87**
Boulder	RMSE	1.317	1.085	1.8	1.3	1.77	**0.71**	0.893
	MAPE	261.4	250.09	325.73	315.86	254.87	**203.71**	245.24
	MSE	1.74	1.16	1.064	1.22	1.16	0.86	**0.8**
Dundee	RMSE	2.30	1.20	1.52	1.5	1.59	**1.13**	1.195
	MAPE	154.74	**100.23**	111.17	117.57	118.61	108.88	102.5
	MSE	6.70	1.44	1.83	2.2	1.27	**1.22**	1.41
Perth	RMSE	1.717	1.35	1.606	1.372	1.386	**1.2**	1.22
	MAPE	114.09	95.37	109.63	103.69	123.81	95.47	**94.96**
	MSE	2.96	1.83	2.557	1.954	1.842	1.76	**1.49**

1) DATA ACQUISITION AND DATA COLLECTION

Reliable, quicker, and more effective communication has emerged during the last few years as a critical component of the smart city implementation. Understanding the potential effects of EV charging on the electrical system is the key goal. Vehicle-to-infrastructure, vehicle-to-vehicle, and vehicle-to-pedestrian are all parts of V2X. V2X communication infrastructure utilizes the technologies like IoT, 5G, and LoRa for the transfer of the data packets [66]. The aggregator or the utilities collect data inferring the customer EV charging and usage patterns in order to inform future schedules and prices.

2) DATA CLEANING AND AGGREGATION

After collecting the data from different devices using the communication infrastructure, it might be difficult to examine unstructured data in such formats since it can be stored in a variety of sources. Data warehouses are used as a result. A data warehouse is a hub where data is consolidated from several databases. To find and eliminate false or corrupted data from the dataset, the data cleaning method is used. The raw data needs cleaning to improve the data consistency to train the model for making the prediction. This step is necessary because the raw data have a lot of noisy datapoints and missing data. In other words, data cleaning aids the overall data analysis. The next step after cleaning is data aggregation which is often used to provide statistical analysis of data to create useful summary data for further analysis.

3) DATA RESAMPLING AND DATA TRANSFORMATION

The dataset is framed in this study to downsample the hourly frequency of power consumption to total daily consumptions, which decreases the data samples of the aggregated load on a daily basis as compared to the original dataset. Energy usage is used for training purposes as a single variable. This approach bases its preprocessing on the target horizon that will be anticipated. This work is associated with daily power consumption predictions, which require the aggregated daily load. The `resample` () is a method of the Pandas dataframes that can be used to summarize data by date or time. Therefore, the `resample` () method together with sum () is evoked by passing the argument 'D' which allows the data indexed by datetime to be grouped by adding up all values for each resampling period, i.e., day in this case [67].

The data normalization step is employed after the data resampling step has been completed. The purpose is to adjust the numerical differences among the data points by scaling each input variable separately by subtracting the mean and dividing by the standard deviation to shift the distribution such that the mean equals zero and the standard deviation equals one. Due to the substantial variances in the target data, the standardization technique aids in enhancing the performance of the model training process and speeds up training [68]. To start training the deep learning model, training data and testing data need to be transformed in the same way. The data standardization is formulated as presented in equation (29):

$$z = \frac{x - \mu}{\sigma} \tag{20}$$

where x is an original value, μ is the mean value of x, σ is the standard deviation of the dataset and z is the normalized value. Data transformation using the standardization removes the mean and scales each feature/variable to unit variance. This operation is performed feature-wise in an independent way. Mean μ and standard deviation σ and standard deviation

$$\mu = {}^{1}/_{N} \sum_{i=1}^{N} (x_i) \tag{21}$$

$$\sigma = \sqrt{{}^{1}/_{N} \sum_{i=1}^{N} (x_i - \mu)^2} \tag{22}$$

4) DATASET FORMATION

After going through all of the above processes of cleaning, resampling, and standardizing, the data is now liable for the deep learning models to be trained. Dataset obtained after the

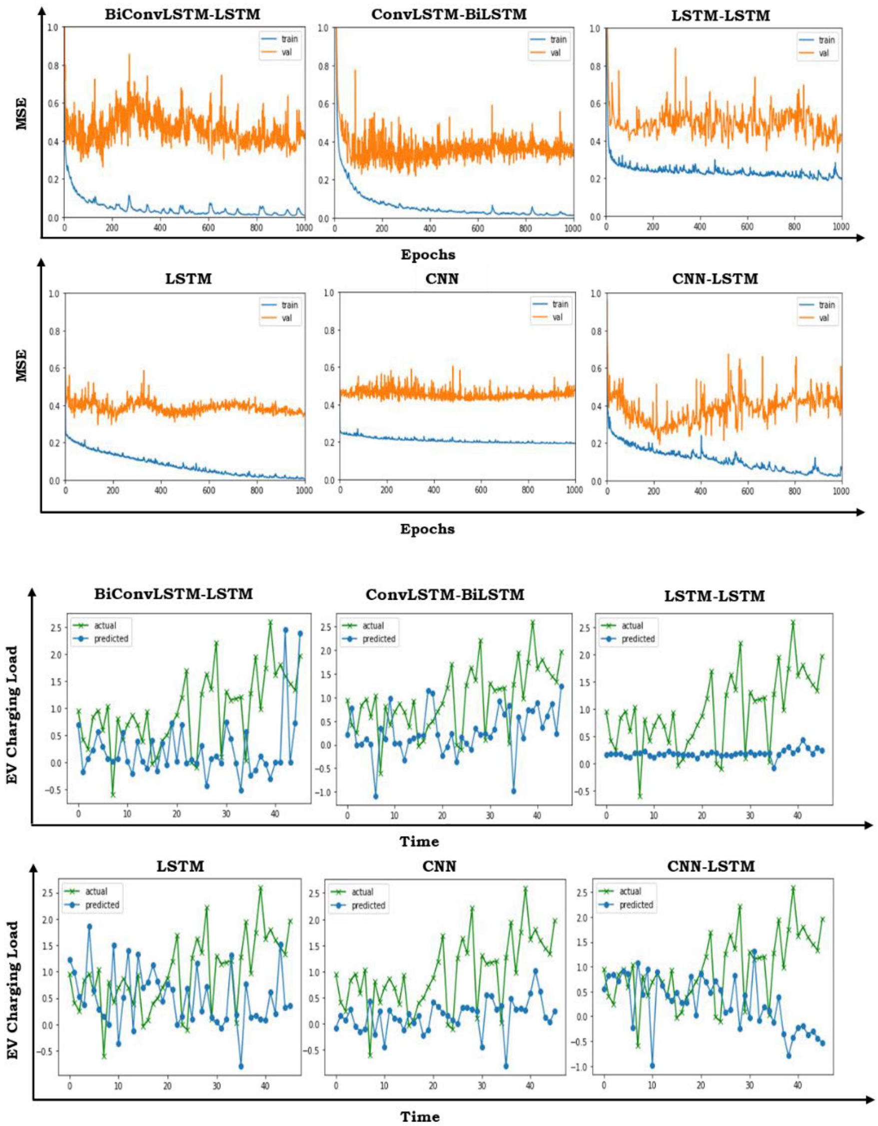

FIGURE 10. Illustration of training loss and validation loss using different architectures for the Palo Alto dataset, and lower figure shows the predicted vs actual charging demand.

preprocessing step is completely a kind of time series data which follows a particular trend. All the variables, including feature vectors as well as target variables, are sequentially recorded data points at regular intervals having a frequency depending upon the time horizon, which may typically be hourly, daily, weekly, monthly, and yearly. As this study revolves around daily energy forecasting but the actual data is non-uniformly distributed hourly electricity data, which implies that after going through all the data preprocessing, the final dataset size has been reduced. In the case of Boulder City, the actual data points are 65,272, and the final preprocessed dataset has 1,431 data points.

C. EXPERIMENTAL RESULTS AND DISCUSSION

This section provides the experimental results of the ConvLSTM and BiConvLSTM based architectures in case of daily energy demand forecasting for electric vehicle charging stations. For the elucidation ***ConvLSTM−BiLSTM*** is represented as proposed model-I and ***BiConvLSTM − LSTM*** as proposed model-II. In Figure 10, the training and validation curves depicts the generalization potential of all the models, where the orange curve represents validation loss and the blue curve for training loss. This is given as MSE metric. Further, it provides visual graphs which depict how strongly the forecasting curve follows the actual curve over a test sample for a week. While as Table 2, provides the results of the two proposed models which are compared with the five conventional models namely LSTM, CNN, CNN-LSTM, LSTM-LSTM, and BiLSTM-BiLSTM. The performance of the proposed models on the four different datasets is evaluated using the MAPE, RMSE, and MSE.

In the case of Palo Alto dataset, the proposed model-I manages to decrease the RMSE by about 23.41%, 23.74%, 34.56%, 38.63%, 20.13%, and 2.74% compared to the

TABLE 3. Description of datasets.

Field Name	Field Type	Description	Palo Alto	Boulder	Dundee	Perth
Station Name	Text	Name of the Charging Station	✓	✓		
Station Address	Text	Address of the charging station		✓	✓	✓
Station Id	Numeric	Charging Session Id			✓	✓
MAC Address	Alphanumeric	MAC address of the CS	✓			
Org Name	Text	Organization Name	✓		✓	
Start Date	Timestamp	Arrival Date and Time of the Charging Session	✓	✓	✓	✓
Start Time Zone	Timestamp	Time Zone of the Charging Session	✓	✓	✓	✓
End Date	Timestamp	End Date and Time of the Charging Session	✓	✓	✓	✓
End Time Zone	Timestamp	Time Zone of the Charging Session	✓	✓	✓	✓
Transaction Date (Pacific Time)	Timestamp	Start Date and Time of the Charging Session	✓	✓	✓	✓
Total Duration (hh:mm: ss)	Timestamp	Total Stay Duration at the Charging Station	✓			
Charging Time (hh:mm: ss)	Timestamp	Total Charging Duration of the Charging Session	✓	✓		
Energy (kWh)	Numeric	Total Energy (kWh) transferred	✓	✓	✓	✓
GHG Savings (kg)	Numeric	Estimated emissions avoided based on the energy dispensed and gasoline saved by the charging stations on the listed date kilograms (kg) of carbon dioxide equivalent (CO_2e)	✓	✓		
Gasoline Savings (gallons)	Numeric	Estimated gallons of gasoline saved based on charging time on the particular listed date	✓	✓		
Port Type	Numeric	The power level of the charging port	✓	✓	✓	✓
Port Number	Numeric	Port Number dedicated to charging (1, 2)	✓		✓	✓
Plug Type	Alphanumeric	Plug Type dedicated to Charging (J1772, NEMA 5-20R)	✓			
Address 1	Text	Address of Charging Station	✓			
City	Text	City in which charging station is located	✓	✓		
State/Province	Text	State in which charging station is located	✓	✓		
Postal Code	Numeric	Zip code for where the charging station is located	✓	✓		
Country	Text	Country in which charging station is located	✓			
Latitude	Numeric	Latitude of the Charging Station	✓			
Longitude	Numeric	Longitude of the Charging Station	✓			
Currency/ Cost	Numeric	USD/ UK Pounds	✓		✓	
Ended By	Text	Charging Session ended through	✓			
Plug-in Event Id	Numeric	Charging Session plug-in event Id	✓			
Driver Postal Code	Numeric	Driver personal Zip code	✓			
User ID	Numeric	EV user Id	✓			

CNN-LSTM, LSTM-LSTM, BiLSTM-BiLSTM, and its variant proposed model-II respectively. Likewise, when we evaluated MSE, it continued to hold an upper hand over the other models, while in terms of MAPE, the proposed model-II manages a superior performance. In the case of the Boulder dataset, the proposed model I continues to outperform in terms of RMSE with respect to other models with a mark of 46.09%, 34.56%, 60.56%, 45.38%, 59.89%, and 20.49%, similarly it manages to potentially reduce MAPE with a percentage of 22.07%, 18.54%, 37.46%, 35.5%, 20.07%, and 16.93% respectively. In terms of MSE, the proposed model-II performs better by achieving 54.02%, 49.04%, 24.81%, 34.21%, 31.21%, and 6.65% decrease compared to other models. In the case of the Dundee dataset, the proposed model-I improves the performance by 25.43% and 33.3% as compared to the CNN-LSTM model, in terms of RMSE and MSE respectively. While as in terms of MAPE, the CNN outperforms all other models followed by proposed model-II. In the case of the Perth dataset, after forecasting the aggregated EV energy consumption for daily basis, the proposed model-I stands first by having 30.23%, 11.11%, 25.28%, 12.54%, 13.42%, and 1.64% least error rate in terms of RMSE comparing to other listed models. Proposed model-II shows remarkable performance in terms

TABLE 4. Comparison of LSTM based encoder-decoder models in terms of RMSE, MAPE, and MSE.

Dataset	Metric	Model				
		2LSTM + LSTM	2LSTM + 2LSTM	LSTM + BiLSTM	2BiLSTM + 2BiLSTM	2LSTM + 2BiLSTM
Palo Alto	RMSE	1.01	1.07	0.957	**0.947**	0.97
	MAPE	218.914	**195**	248.3	238.9	207.9
	MSE	0.927	**0.92**	0.93	0.943	0.967
Boulder	RMSE	1.27	0.993	1.062	1.83	**0.915**
	MAPE	**261.271**	282.1	275.614	262.59	268.76
	MSE	1.01	0.985	1.11	1.116	**0.894**
Dundee	RMSE	1.347	1.585	1.655	**1.275**	1.302
	MAPE	105.085	**101.8**	118.6	102.786	178.31
	MSE	1.829	1.66	2.843	**1.386**	1.685
Perth	RMSE	1.293	1.256	1.606	1.279	**1.193**
	MAPE	96.342	94.657	101.386	100.27	**92.642**
	MSE	**1.4**	1.471	2.586	1.54	1.429

TABLE 5. Comparison of CNN and LSTM based encoder-decoder models in terms of RMSE, MAPE, and MSE.

Dataset	Metric	Model			
		CNN + LSTM	2CNN* + 2LSTM	CNN + BiLSTM	2CNN + 2BiLSTM
Palo Alto	RMSE	1	**0.91**	0.97	0.884
	MAPE	262.8	234.81	295.7	**208.6**
	MSE	1.066	0.903	0.977	**0.802**
Boulder	RMSE	1.099	1.17	**1.025**	1.38
	MAPE	290.214	**291.9**	310.057	297.1
	MSE	1.2	1.11	**1.029**	1.12
Dundee	RMSE	1.33	**1.14**	1.448	1.476
	MAPE	168.514	111.89	115.17	**109.286**
	MSE	1.4	**1.259**	2.1	1.871
Perth	RMSE	1.44	**1.34**	1.553	1.67
	MAPE	109.46	104.87	**102.5**	117.47
	MSE	**1.785**	1.87	2.3	2.4

TABLE 6. Comparison of ConvLSTM and BiConvLSTM based encoder-decoder models in terms of RMSE, MAPE, and MSE.

Dataset	Metric	Model							
		ConvLSTM + LSTM	ConvLSTM + 2LSTM*	ConvLSTM + 3LSTM	2ConvLSTM + 2LSTM	ConvLSTM + BiLSTM	ConvLSTM + 2BiLSTM	BiConvLSTM + LSTM	2BiConvLSTM + BiLSTM
Palo Alto	RMSE	0.98	1.239	1.202	0.916	1.01	0.74	**0.97**	1.07
	MAPE	307.1	310.31	269.34	264.3	291.67	455.886	**260.557**	292
	MSE	1.01	1.542	1.429	0.857	1.28	0.97	**0.91**	12.11
Boulder	RMSE	**0.72**	1.183	0.959	1.184	1.079	0.77	0.933	0.867
	MAPE	353.4	291.871	278.629	268.64	**256.9**	278.2	307.8	367.97
	MSE	0.892	1.029	0.943	1.348	1.1	**0.886**	1.31	1.44
Dundee	RMSE	1.23	1.164	**1.138**	1.234	1.24	1.289	1.265	1.27
	MAPE	104.13	104.371	**103.01**	103.557	116.47	106.63	106.37	121.57
	MSE	1.51	1.343	1.914	1.5	**1.273**	1.84	1.6	1.99
Perth	RMSE	1.68	1.257	1.212	1.28	1.319	1.549	**1.191**	1.531
	MAPE	97.7	**93.73**	99.26	103.17	106.79	105.343	98.6	111.843
	MSE	2.842	1.71	1.47	1.66	1.59	1.83	1.793	**1.282**

of MAPE and MSE by attaining the value of 94.96 and 1.49 respectively which much less as compared to conventional models. Overall the two proposed models outperforms the conventional state-of-art encoder-decoder based deep learning models, proposed model-I followed by the proposed model-II.

To create the deep learning models, we combined the Keras library with TensorFlow in the backend [69]. The NVIDIA GeForce GTX 970 graphics card, Intel Core i7 processor with 8 GB RAM and Microsoft Windows 10 operating system were used for all the trials.

D. ABLATION STUDY

In order to select the feasible model architectures for the forecasting task, we employed several deep learning architectures to confirm the best model. We examine the effects of changing the number of layers in the encoder as well as the decoder network by implementing different versions of the baseline models to validate the generalization of the proposed models. To improve the performance, by changing the number of layers the error is reduced by a good percentage as compared to considered baseline models of the LSTM-LSTM, BiLSTM-BiLSTM and CNN-LSTM. All the experimental results are given in the appendix section Table 4 and Table 5. While as Table 6, depicts the prediction error of the different versions ConvLSTM and BiConvLSTM based architectures. The average output results of the two proposed models as compared to the results of the modified baseline architectures as well as their own modified versions are still outstanding.

VI. CONCLUSION

This work proposed two unique encoder-decoder based deep learning architectures called ConvLSTM and BiConvLSTM, to overcome the challenges of energy demand forecasting for the network of electric vehicle charging stations. Datasets from four locations (two regions in the UK and two in the USA) were used. Several benchmark algorithms were also contrasted with the suggested method in order to judge the robustness of the proposed approach. The effectiveness of these forecasting systems have been evaluated using three error metrics: RMSE, MSE, and MAPE. The acquired findings showed that the suggested models outperformed the benchmarks. For example, considering all the four datasets the average performance of the two proposed models (*proposed model-I* and *proposed model-II*) versus other state-of-art models was 33.31% and 28.19% better in terms of RMSE. Further improvement to enhance the performance of the suggested models could be done by using hyperparameter tuning techniques of the deep learning architectures, by using multi-variate EVCS dataset including average daily drive, and charging cost, and residential EV energy demand dataset.

APPENDIX

See Tables 3–6.

REFERENCES

[1] IEA, Paris, France. (2022). *Global EV Outlook 2022*. [Online]. Available: https://www.iea.org/reports/global-ev-outlook-2022

[2] C. Feng, Y. Wang, Q. Chen, Y. Ding, G. Strbac, and C. Kang, "Smart grid encounters edge computing: Opportunities and applications," *Adv. Appl. Energy*, vol. 1, Feb. 2021, Art. no. 100006, doi: 10.1016/j.adapen.2020.100006.

[3] D. Sun, Q. Ou, X. Yao, S. Gao, Z. Wang, W. Ma, and W. Li, "Integrated human-machine intelligence for EV charging prediction in 5G smart grid," *EURASIP J. Wireless Commun. Netw.*, vol. 2020, no. 1, p. 139, Dec. 2020.

[4] C. B. Heendeniya and L. Nespoli, "A stochastic deep reinforcement learning agent for grid-friendly electric vehicle charging management," *Energy Informat.*, vol. 5, no. S1, pp. 1–14, Sep. 2022, doi: 10.1186/s42162-022-00197-5.

[5] *Society of Automotive Engineers*. Accessed: Jan. 10, 2023. [Online]. Available: https://www.sae.org/news/2022/03/maintaining-ev-chargers-another-challenge

[6] E. El Ghanam, M. Hassan, A. Osman, and I. Ahmed, "Review of communication technologies for electric vehicle charging management and coordination," *World Electr. Vehicle J.*, vol. 12, no. 3, p. 92, Jun. 2021, doi: 10.3390/wevj12030092.

[7] V. S. R. Tappeta, B. Appasani, S. Patnaik, and T. S. Ustun, "A review on emerging communication and computational technologies for increased use of plug-in electric vehicles," *Energies*, vol. 15, no. 18, p. 6580, Sep. 2022, doi: 10.3390/en15186580.

[8] L. N. Cain and A. Lastuka, "Forecasting demand for electric vehicle charging infrastructure: Definitions, assumptions and conceptual models," Center Sustain. Energy, San Diego, CA, USA, Tech. Rep., May 2021.

[9] S. Shahriar, A. R. Al-Ali, A. H. Osman, S. Dhou, and M. Nijim, "Machine learning approaches for EV charging behavior: A review," *IEEE Access*, vol. 8, pp. 168980–168993, 2020, doi: 10.1109/access.2020.3023388.

[10] Y. Lu, Y. Li, D. Xie, E. Wei, X. Bao, H. Chen, and X. Zhong, "The application of improved random forest algorithm on the prediction of electric vehicle charging load," *Energies*, vol. 11, no. 11, p. 3207, Nov. 2018, doi: 10.3390/en11113207.

[11] D.-H. Lee, M.-S. Kim, J.-H. Roh, J.-P. Yang, and J.-B. Park, "Forecasting of electric vehicles charging pattern using Bayesians method with the convolustion," *IFAC-PapersOnLine*, vol. 52, no. 4, pp. 413–418, 2019.

[12] S. Grubwinkler and M. Lienkamp, "Energy prediction for EVs using support vector regression methods," in *Intelligent Systems* (Advances in Intelligent Systems and Computing), vol. 323. Cham, Switzerland: Springer, 2014, doi: 10.1007/978-3-319-11310-4_67.

[13] J. Ge, M. Li, H. Xie, J. Bai, L. Li, and P. Huang, "Multi-time scale prediction method of electric vehicle charging load based on support vector machine," in *Proc. 7th Int. Symp. Adv. Electr., Electron., Comput. Eng.*, Oct. 2022, Art. no. 122945G, doi: 10.1117/12.2641265.

[14] A. Poghosyan, D. V. Greetham, S. Haben, and T. Lee, "Long term individual load forecast under different electrical vehicles uptake scenarios," *Appl. Energy*, vol. 157, pp. 699–709, Nov. 2015.

[15] M. Majidpour, C. Qiu, P. Chu, H. R. Pota, and R. Gadh, "Forecasting the EV charging load based on customer profile or station measurement?" *Appl. Energy*, vol. 163, pp. 134–141, Feb. 2016.

[16] C. Gomez-Quiles, G. Asencio-Cortes, A. Gastalver-Rubio, F. Martinez-Alvarez, A. Troncoso, J. Manresa, J. C. Riquelme, and J. M. Riquelme-Santos, "A novel ensemble method for electric vehicle power consumption forecasting: Application to the Spanish system," *IEEE Access*, vol. 7, pp. 120840–120856, 2019.

[17] S. M. J. Jalali, S. Ahmadian, A. Khosravi, M. Shafie-Khah, S. Nahavandi, and J. P. S. Catalao, "A novel evolutionary-based deep convolutional neural network model for intelligent load forecasting," *IEEE Trans. Ind. Informat.*, vol. 17, no. 12, pp. 8243–8253, Dec. 2021.

[18] F. Mohammad, M. A. Ahmed, and Y.-C. Kim, "Efficient energy management based on convolutional long short-term memory network for smart power distribution system," *Energies*, vol. 14, no. 19, p. 6161, Sep. 2021.

[19] L. Semmelmann, S. Henni, and C. Weinhardt, "Load forecasting for energy communities: A novel LSTM-XGBoost hybrid model based on smart meter data," *Energy Informat.*, vol. 5, no. S1, pp. 1–21, Sep. 2022, doi: 10.1186/s42162-022-00212-9.

[20] Y. Xie, Y. Ueda, and M. Sugiyama, "A two-stage short-term load forecasting method using long short-term memory and multilayer perceptron," *Energies*, vol. 14, no. 18, p. 5873, Sep. 2021, doi: 10.3390/en14185873.

[21] N. Khan, I. U. Haq, S. U. Khan, S. Rho, M. Y. Lee, and S. W. Baik, "DB-net: A novel dilated CNN based multi-step forecasting model for power consumption in integrated local energy systems," *Int. J. Electr. Power Energy Syst.*, vol. 133, Dec. 2021, Art. no. 107023.

[22] Y. Kim and S. Kim, "Forecasting charging demand of electric vehicles using time-series models," *Energies*, vol. 14, no. 5, p. 1487, Mar. 2021, doi: 10.3390/en14051487.

[23] J. Zhu, Z. Yang, Y. Guo, J. Zhang, and H. Yang, "Short-term load forecasting for electric vehicle charging stations based on deep learning approaches," *Appl. Sci.*, vol. 9, no. 9, p. 1723, 2019, doi: 10.3390/app9091723.
[24] J. Zhu, Z. Yang, M. Mourshed, Y. Guo, Y. Zhou, Y. Chang, Y. Wei, and S. Feng, "Electric vehicle charging load forecasting: A comparative study of deep learning approaches," *Energies*, vol. 12, no. 14, p. 2692, Jul. 2019, doi: 10.3390/en12142692.
[25] M. Chang, S. Bae, G. Cha, and J. Yoo, "Aggregated electric vehicle fast-charging power demand analysis and forecast based on LSTM neural network," *Sustainability*, vol. 13, no. 24, p. 13783, Dec. 2021, doi: 10.3390/su132413783.
[26] J. Shanmuganathan, A. A. Victoire, G. Balraj, and A. Victoire, "Deep learning LSTM recurrent neural network model for prediction of electric vehicle charging demand," *Sustainability*, vol. 14, no. 16, p. 10207, Aug. 2022, doi: 10.3390/su141610207.
[27] D. Zhou, Z. Guo, Y. Xie, Y. Hu, D. Jiang, Y. Feng, and D. Liu, "Using Bayesian deep learning for electric vehicle charging station load forecasting," *Energies*, vol. 15, no. 17, p. 6195, Aug. 2022, doi: 10.3390/en15176195.
[28] M. Akil, E. Dokur, and R. Bayindir, "Analysis of electric vehicle charging demand forecasting model based on Monte Carlo simulation and EMD-BO-LSTM," in *Proc. 10th Int. Conf. Smart Grid (icSmartGrid)*, Jun. 2022, pp. 356–362.
[29] X. Huang, D. Wu, and B. Boulet, "Ensemble learning for charging load forecasting of electric vehicle charging stations," in *Proc. IEEE Electr. Power Energy Conf. (EPEC)*, Nov. 2020, pp. 1–5.
[30] X. Zhang, K. W. Chan, H. Li, H. Wang, J. Qiu, and G. Wang, "Deep-learning-based probabilistic forecasting of electric vehicle charging load with a novel queuing model," *IEEE Trans. Cybern.*, vol. 51, no. 6, pp. 3157–3170, Jun. 2021.
[31] L. Buzna, P. De Falco, G. Ferruzzi, S. Khormali, D. Proto, N. Refa, M. Straka, and G. van der Poel, "An ensemble methodology for hierarchical probabilistic electric vehicle load forecasting at regular charging stations," *Appl. Energy*, vol. 283, Feb. 2021, Art. no. 116337.
[32] F. B. Hüttel, I. Peled, F. Rodrigues, and F. C. Pereira, "Deep spatio-temporal forecasting of electrical vehicle charging demand," 2021, *arXiv:2106.10940*.
[33] Y. M. Saputra, D. T. Hoang, D. N. Nguyen, E. Dutkiewicz, M. D. Mueck, and S. Srikanteswara, "Energy demand prediction with federated learning for electric vehicle networks," in *Proc. IEEE Global Commun. Conf. (GLOBECOM)*, Dec. 2019, pp. 1–6.
[34] Q. Xing, Z. Chen, Z. Zhang, X. Huang, Z. Leng, K. Sun, Y. Chen, and H. Wang, "Charging demand forecasting model for electric vehicles based on online ride-hailing trip data," *IEEE Access*, vol. 7, pp. 137390–137409, 2019.
[35] Q. Xing, Z. Chen, Z. Zhang, X. Xu, T. Zhang, X. Huang, and H. Wang, "Urban electric vehicle fast-charging demand forecasting model based on data-driven approach and human decision-making behavior," *Energies*, vol. 13, no. 6, p. 1412, Mar. 2020.
[36] J. Zhang, F. Xu, Y. Zhang, and T. Shen, "ELM-based driver torque demand prediction and real-time optimal energy management strategy for HEVs," *Neural Comput. Appl.*, vol. 32, no. 18, pp. 14411–14429, Sep. 2020.
[37] H. M. Abdullah, A. Gastli, and L. Ben-Brahim, "Reinforcement learning based EV charging management Systems–A review," *IEEE Access*, vol. 9, pp. 41506–41531, 2021, doi: 10.1109/access.2021.3064354.
[38] M. Dabbaghjamanesh, A. Moeini, and A. Kavousi-Fard, "Reinforcement learning-based load forecasting of electric vehicle charging station using Q-learning technique," *IEEE Trans. Ind. Informat.*, vol. 17, no. 6, pp. 4229–4237, Jun. 2021, doi: 10.1109/TII.2020.2990397.
[39] X. Shi, Z. Chen, H. Wang, D.-Y. Yeung, W.-K. Wong, and W.-C. Woo, "Convolutional LSTM network: A machine learning approach for precipitation nowcasting," in *Proc. NIPS*, 2015, pp. 1–9.
[40] H. Song, W. Wang, J. Shen, S. Zhao, and K. M. Lam, "Pyramid dilated deeper ConvLSTM for video salient object detection," in *Proc. Eur. Conf. Comput. Vis. (ECCV)*, 2018, pp. 715–731.
[41] R. Azad, M. Asadi-Aghbolaghi, M. Fathy, and S. Escalera, "Bi-directional ConvLSTM U-Net with densley connected convolutions," in *Proc. IEEE/CVF Int. Conf. Comput. Vis. Workshop (ICCVW)*, Oct. 2019, pp. 406–415.
[42] A. Hanson, P. N. V. R. Koutilya, S. Krishnagopal, and L. Davis, "Bidirectional convolutional LSTM for the detection of violence in videos," in *Proc. ECCV Workshops*, 2018, pp. 280–295.
[43] Z. Liu, Q. Wu, M. Shahidehpour, C. Li, S. Huang, and W. Wei, "Transactive real-time electric vehicle charging management for commercial buildings with PV on-site generation," *IEEE Trans. Smart Grid*, vol. 10, no. 5, pp. 4939–4950, Sep. 2019.
[44] S. Baik, Y. Jin, and Y. Yoon, "Determining equipment capacity of electric vehicle charging station operator for profit maximization," *Energies*, vol. 11, no. 9, p. 2301, Sep. 2018, doi: 10.3390/en11092301.
[45] D. Aguilar-Dominguez, J. Ejeh, A. D. F. Dunbar, and S. F. Brown, "Machine learning approach for electric vehicle availability forecast to provide vehicle-to-home services," *Energy Rep.*, vol. 7, pp. 71–80, May 2021.
[46] W. Zhang, H. Liu, J. Han, Y. Ge, and H. Xiong, "Multi-agent graph convolutional reinforcement learning for dynamic electric vehicle charging pricing," in *Proc. 28th ACM SIGKDD Conf. Knowl. Discovery Data Mining*. New York, NY, USA: Association for Computing Machinery, Aug. 2022, pp. 2471–2481, doi: 10.1145/3534678.3539416.
[47] S. Aznavi, P. Fajri, M. B. Shadmand, and A. Khoshkbar-Sadigh, "Peer-to-peer operation strategy of PV equipped office buildings and charging stations considering electric vehicle energy pricing," *IEEE Trans. Ind. Appl.*, vol. 56, no. 5, pp. 5848–5857, Sep. 2020.
[48] M. Adil, M. A. P. Mahmud, A. Z. Kouzani, and S. Khoo, "Energy trading among electric vehicles based on Stackelberg approaches: A review," *Sustain. Cities Soc.*, vol. 75, Dec. 2021, Art. no. 103199, doi: 10.1016/j.scs.2021.103199.
[49] S. Englberger, K. A. Gamra, B. Tepe, M. Schreiber, A. Jossen, and H. Hesse, "Electric vehicle multi-use: Optimizing multiple value streams using mobile storage systems in a vehicle-to-grid context," *Appl. Energy*, vol. 304, Dec. 2021, Art. no. 117862, doi: 10.1016/j.apenergy.2021.117862.
[50] P. Chakraborty, R. Parker, T. Hoque, J. Cruz, L. Du, S. Wang, and S. Bhunia, "Addressing the range anxiety of battery electric vehicles with charging en route," *Sci. Rep.*, vol. 12, no. 1, p. 5588, Apr. 2022, doi: 10.1038/s41598-022-08942-2.
[51] H. A. Ozkan and M. Erol-Kantarci, "A novel electric vehicle charging/discharging scheme with incentivization and complementary energy sources," *J. Energy Storage*, vol. 51, Jul. 2022, Art. no. 104493, doi: 10.1016/j.est.2022.104493.
[52] J. Zhang, F.-Y. Wang, K. Wang, W.-H. Lin, X. Xu, and C. Chen, "Data-driven intelligent transportation systems: A survey," *IEEE Trans. Intell. Transp. Syst.*, vol. 12, no. 4, pp. 1624–1639, Dec. 2011, doi: 10.1109/tits.2011.2158001.
[53] Y. Amara-Ouali, Y. Goude, B. Hamrouche, and M. Bishara, "A benchmark of electric vehicle load and occupancy models for day-ahead forecasting on open charging session data," in *Proc. 13th ACM Int. Conf. Future Energy Syst.*, Jun. 2022, pp. 193–207.
[54] Y. Amara-Ouali, P. Massart, J.-M. Poggi, Y. Goude, and H. Yan, "A review of electric vehicle charging session open data," in *Proc. 12th ACM Int. Conf. Future Energy Syst.*, Jun. 2021, pp. 278–279.
[55] C. Hecht, J. Figgener, and D. U. Sauer, "Simultaneity factors of public electric vehicle charging stations based on real-world occupation data," *World Electr. Vehicle J.*, vol. 13, no. 7, p. 129, Jul. 2022.
[56] M. F. Elahe, M. Jin, and P. Zeng, "Knowledge-based systematic feature extraction for identifying households with plug-in electric vehicles," *IEEE Trans. Smart Grid*, vol. 13, no. 3, pp. 2259–2268, May 2022.
[57] City of Palo Alto. (2021). *Electric Vehicle Charging Station Usage (July 2011-Dec 2020). Open Data. City of Palo Alto.* [Online]. Available: https://data.cityofpaloalto.org/dataviews/257812/electric-vehicle-charging-station-usage-july-2011-dec-2020/
[58] Boulder, CO, USA. *Electric Vehicle Charging Station Energy Consumption*. Accessed: Jan. 10, 2023. [Online]. Available: https://opendata.bouldercolorado.gov/datasets/39288b03f8d54b39848a2df9f1c5fca2_0/explore
[59] City of Dundee. (Mar. 2019). *Electric Vehicle Charging Sessions Dundee*. [Online]. Available: https://data.dundeecity.gov.uk/dataset/ev-charging-data
[60] Perth and Kinross. (Oct. 2020). *Electric Vehicle Charging Station Usage*. [Online]. Available: https://data.pkc.gov.uk/dataset/ev-charging-data
[61] *Data Collection on Charging Patterns Among Top 2018 EV Trends: Report*. Accessed: Jan. 10, 2023. [Online]. Available: https://www.publicpower.org/periodical/article/data-collection-charging-patterns-among-top-2018-ev-trends-report
[62] A. Thingvad, "The role of electric vehicles in global power systems," Ph.D. thesis, Tech. Univ. Denmark, Lyngby, Denmark, 2021. [Online]. Available: https://orbit.dtu.dk/en/publications/the-role-of-electric-vehicles-in-global-power-systems

[63] K. Schwenk, "A smart charging assistant for electric vehicles considering battery degradation, power grid and user constraints," Ph.D. thesis, Karlsruhe Inst. Technol. (KIT), Karlsruhe, Germany, 2020.

[64] K. Cho, B. van Merrienboer, C. Gulcehre, D. Bahdanau, F. Bougares, H. Schwenk, and Y. Bengio, "Learning phrase representations using RNN encoder–decoder for statistical machine translation," in *Proc. Conf. Empirical Methods Natural Lang. Process. (EMNLP)*, 2014, pp. 1724–1734.

[65] *How to Backtest Machine Learning Models for Time Series Forecasting*. Accessed: Jan. 10, 2023. [Online]. Available: https://machinelearningmastery.com/backtest-machine-learning-models-time-series-forecasting/

[66] J. L. Gallardo, M. A. Ahmed, and N. Jara, "LoRa IoT-based architecture for advanced metering infrastructure in residential smart grid," *IEEE Access*, vol. 9, pp. 124295–124312, 2021, doi: 10.1109/access.2021.3110873.

[67] *Resample Time Series Data Using Pandas Dataframes*. Accessed: Jan. 10, 2023. [Online]. Available: https://www.earthdatascience.org/courses/use-data-open-source-python/use-time-series-data-in-python/date-time-types-in-pandas-python/resample-time-series-data-pandas-python/

[68] *Data Standardization*. Accessed: Jan. 10, 2023. [Online]. Available: https://www.sisense.com/glossary/data-standardization/

[69] *TensorFlow*. [Online]. Available: https://www.tensorflow.org/

FAISAL MOHAMMAD received the B.S. degree in computer science and engineering from the University of Kashmir, and the M.S. degree in computer science and engineering from the Department of Computer Science and Engineering, Jeonbuk National University, Jeonju, South Korea, in 2019, where he is currently pursuing the Ph.D. degree in computer science and engineering. During his stay, he was a Researcher with the Advanced Communication and Network Laboratory (ADCAN Laboratory), Jeonbuk National University. His research interests include deep learning, reinforcement learning, smart grids, electric vehicle charging and discharging scheduling, cloud computing, and energy demand forecasting.

DONG-KI KANG received the M.S. degree in computer engineering from Jeonbuk National University, Jeonju, South Korea, in 2011, and the Ph.D. degree in electrical engineering from the Korea Advanced Institute of Technology (KAIST), Daejeon, South Korea. He is currently an Assistant Professor with the Department of Electronics Engineering, Jeonbuk National University. His research interests include cloud computing, deep learning, and GPU power control.

MOHAMED A. AHMED received the B.Sc. and M.Sc. degrees in electrical engineering (electronics and communications) from Minia University, Minia, Egypt, in 2003 and 2007, respectively, and the Ph.D. degree in electronics and information engineering from Jeonbuk National University, Jeonju, South Korea, in 2014. He is currently an Assistant Professor with the Department of Electronic Engineering, Universidad Técnica Federico Santa María (UTFSM), Chile. He is also an Assistant Professor with the Department of Communications and Electronics, Higher Institute of Engineering and Technology-King Marriott, Alexandria, Egypt. Prior to joining UTFSM, he was a Postdoctoral Research Fellow with the Advanced Communication and Network Laboratory (ADCAN), Jeonbuk National University, from 2014 to 2018. His research interests include wireless sensor networks, wind energy, electric vehicles, smart grids, and cyber-physical systems.

YOUNG-CHON KIM received the B.S., M.S., and Ph.D. degrees from Korea University, Seoul, South Korea, in 1980, 1982, and 1987, respectively. He joined the Department of Computer Engineering, Jeonbuk National University, Jeonju, South Korea, in 1986. From 1989 to 1990, he was a Postdoctoral Fellow with the University of California at Irvine, Irvine, CA, USA. From 1998 to 2000, he was a Visiting Researcher with the Network Research Laboratory, University of California at Davis, Davis, CA, USA. He is currently a Professor with the School of Information Technology, Jeonbuk National University. His research interests include high-speed optical communication networks, next generation IP networks, and broadband wireless communication networks. He was awarded the Best Professor from the College of Engineering, Jeonbuk National University, in 2002. He was also awarded the Motorola Academic Excellence Award, in 2003.